LIGO Laboratory / LIGO Scientific Collaboration

LIGO-T070313-00-D *LIGO* Dec 10 2007

Hysteresis in Maraging Springs

Arianna Di Cintio

Distribution of this document:
LIGO Science Collaboration

This is an internal working note
of the LIGO Project.

California Institute of Technology
LIGO Project – MS 18-34
1200 E. California Blvd.
Pasadena, CA 91125
Phone (626) 395-2129
Fax (626) 304-9834
E-mail: info@ligo.caltech.edu

Massachusetts Institute of Technology
LIGO Project – NW17-161
175 Albany St
Cambridge, MA 02139
Phone (617) 253-4824
Fax (617) 253-7014
E-mail: info@ligo.mit.edu

LIGO Hanford Observatory
P.O. Box 1970
Mail Stop S9-02
Richland WA 99352
Phone 509-372-8106
Fax 509-372-8137

LIGO Livingston Observatory
P.O. Box 940
Livingston, LA 70754
Phone 225-686-3100
Fax 225-686-7189

http://www.ligo.caltech.edu/

California Institute of Technology

2007

Hysteresis in Maraging Springs

Student
Arianna Di Cintio
University of Rome "La Sapienza"

Mentor
Riccardo De Salvo
LIGO Project

Contents

Introduction

Seismic and anthropogenic activity are principal sources of low frequency noise for earth-based gravitational waves (GW) detectors.In GW interferometers an incoming wave produced by particular astrophysical events is detected by a change in the optical path length of an interferometer. Typically seismic ground motion is several orders of magnitude greater than the displacement which a GW interferometer must detect, so a seismic isolation is necessary.
The Monolithic Geometric Anti Spring filter was developed to provide vertical attenuation at low frequency. Studying the transfer function of this filter at low resonant frequency, we found an unexplained behaviour: a 1/f trend appears instead of the expected $1/f^2$ .A theory is that the effect may be due to the hysteresis of the springs. This is the starting point of our work. We want to study the hysteresis loop of the maraging anti-spring, mounted on the GAS filter.

GAS filter transfer function

The GAS filter consists of a set of radially-arranged cantilever springs, clamped at the base to a common frame ring and opposing each other via a central disk (fig.1).The payload to be isolated is suspended with a steel wire from the central disk. The clamps can be adjusted to change the blades' radial (horizontal) compression, generating the arbitrarily low effective spring constant and resonant frequency thanks to the resulting Anti-Spring effect (fig.1.1,1.2).

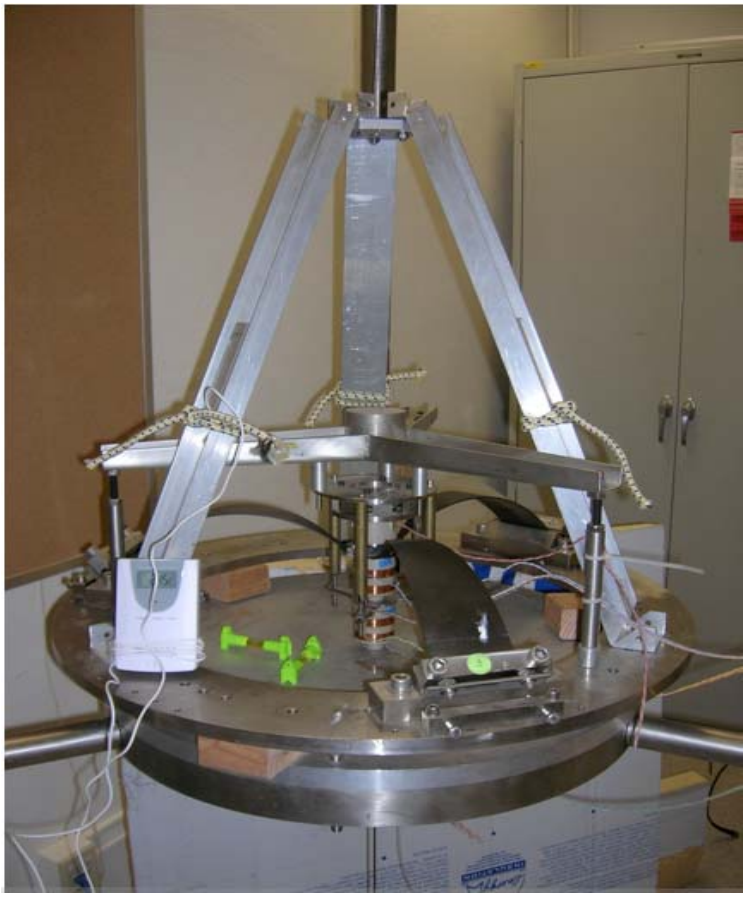

Fig.1: GAS filter

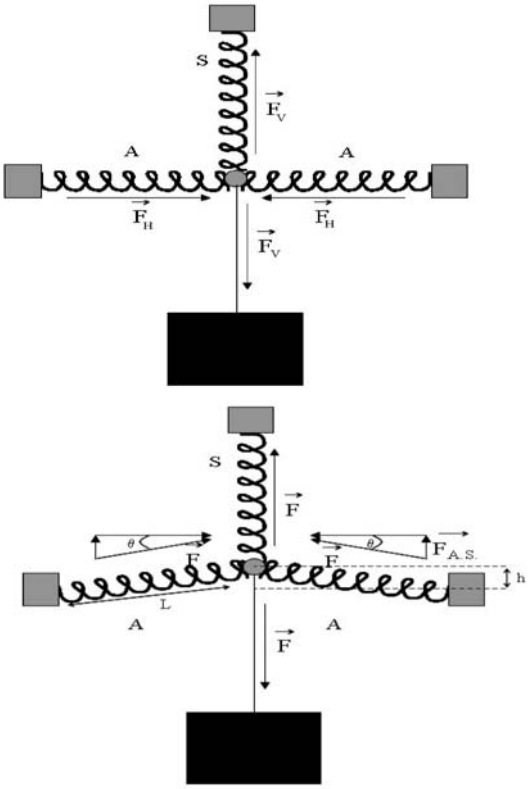

Fig. 1.1: Sketch of the GAS mechanism. At the working point (top sketch) the vertical spring S supports the weight of the payload. The two opposite springs A are compressed, and their forces cancel. Moving out of the working point (bottom sketch) the opposing forces of the A springs do not cancel completely, generating a vertical component proportional to the displacement from the working point, the Anti-Spring force. The opposing springs may be mechanical or magnetic.

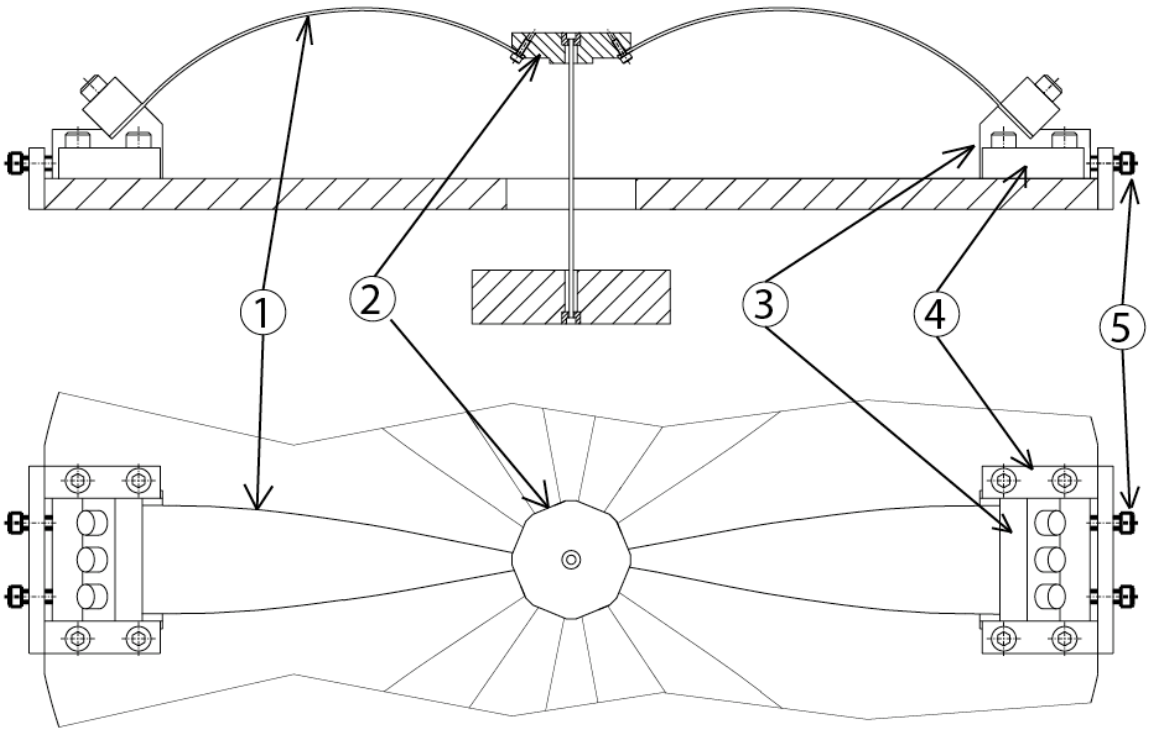

Fig.1.2: Sketch illustrating the GAS mechanism, side and top view. Two (or more) flat blades (1) are pre-stressed (bent cylindrically) and mounted face to face against a keystone (2) which suspends the payload. The blades are held in 45° clamps (3) that can slide into coulisses (4). The radial compression of the blades, governing the Geometric Anti Spring mechanism, is obtained by micrometrically pushing on the blade clamps with tuning screws (5). The blades are cut with a characteristic ogival profile (visible in the top view) so that in working conditions they bend in a perfectly circular arc (side view) and the material is subject to uniform stress.

The GAS works as a normal harmonic oscillator in the vertical direction along which the transfer function is

$$H = \frac{\omega_0^2}{\omega_0^2 - \omega^2}$$

Where $\omega_0^2 = k_{eff} / m$ is the angular frequency of the vertical resonance.

Between the resonant frequency and a critical frequency (due to the distributed mass of the blades) the amplitude of the transfer function reduces proportionally to $1/f^2$: this corresponds to the suppressed transmission of the ground motion to the suspended object (fig.2).

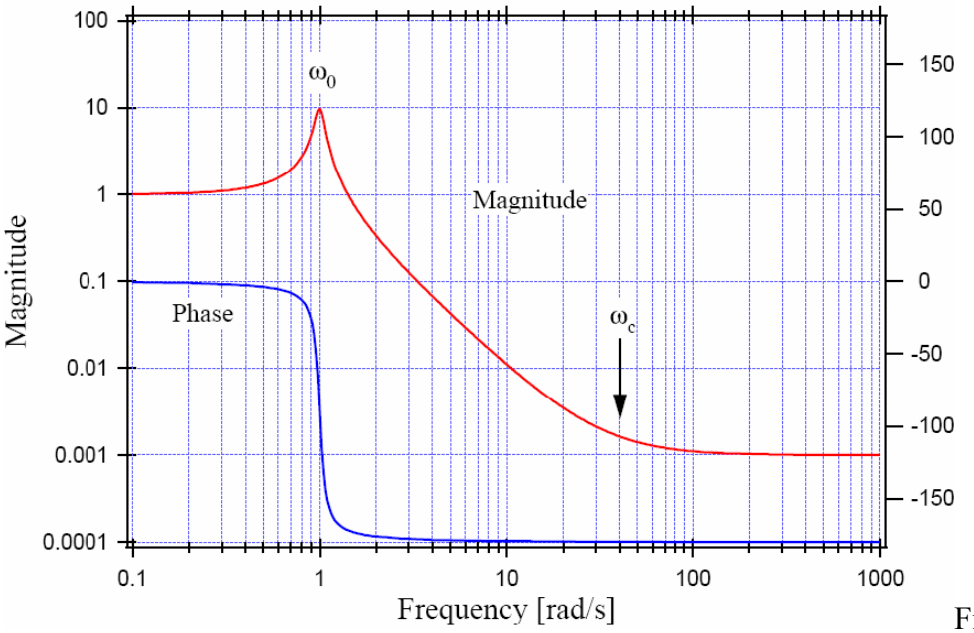

Fig.2:GAS filter transfer function

Looking at the transfer function at resonant frequencies below 100 mHz we found a strange deviation from $1/f^2$: a 1/f trend appears (fig.3), probably due to the hysterisis of the maraging springs.

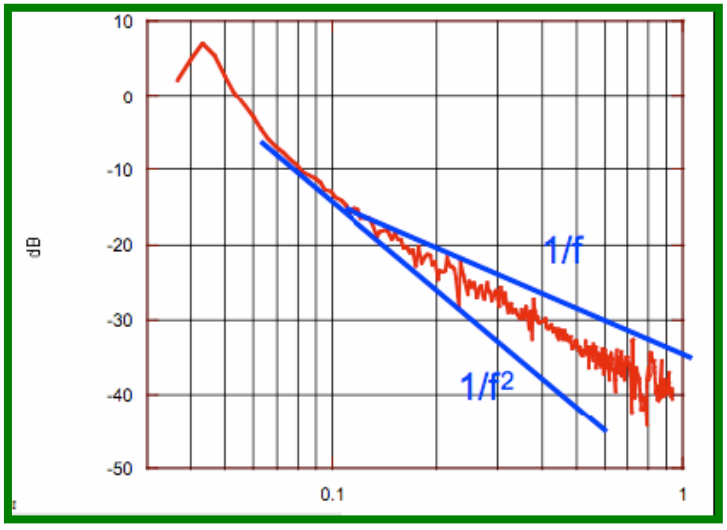

Fig.3:Deviation from $1/f^2$ in the GAS filter transfer function

Hysteresis Theory

To study this effect we want to measure the hysteresis of the springs by applying different forces on the system. We need to acquire measures of the system displacement, using LVDTs sensors, versus forces, applied with an actuator.
If hysteresis'theory is correct we should find a behaviour similar to that of figure 4 for the application of a cyclical force:

Fig.4: Hysteresis cycle

The area of this loop is the lost energy of the system, that is expected to be proportional to the square of the strain times a loss factor.

Measurement Apparatus

The movement of the GAS spring is acquired by means of an LVDT (linear variable differential transformer) position sensor.

An LVDT is constituted by three coaxial coils (fig.5), two large ones in series, coiled on a common rigid spool, but in opposite winding direction, which are mounted on a reference structure and act as a receiver and a smaller coil, which is the emitting coil, positioned between the larger ones and fastened to the moving mechanical component.

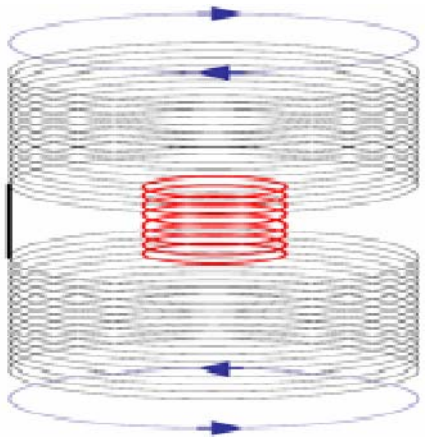

Fig.5:Schematic view of LVDT sensor

We have three LVDTs in the system but we use only one of them.
In our case the reference structure is the GAS filter body and the central emitting coil moves with the payload movement (fig.6).
The central emitting coil is driven by a sinusoidal signal with 20 KHz of frequency. The position measurement is obtained by measuring in a lock-in amplifier the amplitude and sign of the voltage generated in the receiving coils by the little emitting coil. The measured voltage depends on how the magnetic field of the two coils overlap.

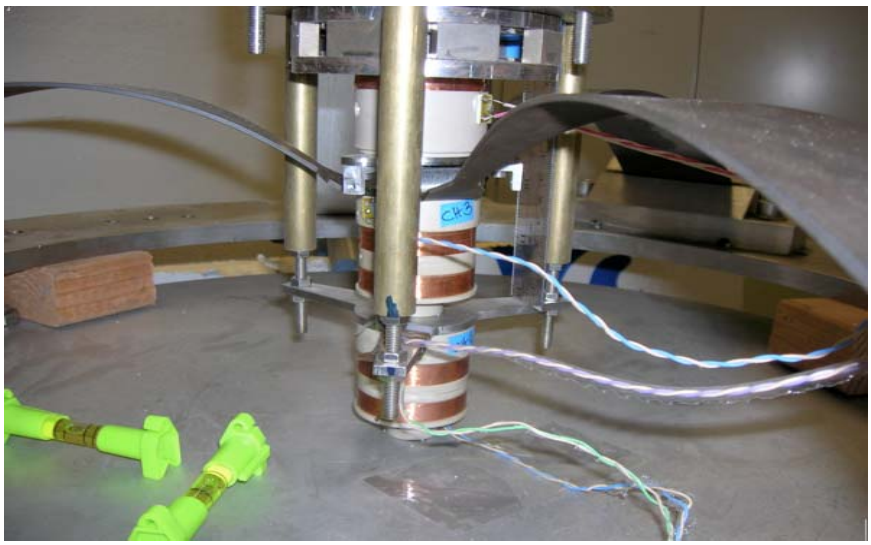

Fig.6:LVDTs on the GAS filter We want to work in the linear range of LVDT sensor and a calibration of this instrument is so necessary. To calibrate LVDT we added coins on the suspended load, acquiring at the same time both voltage (from LVDT) and height of the equilibrium point of the system.
We found this behaviour:

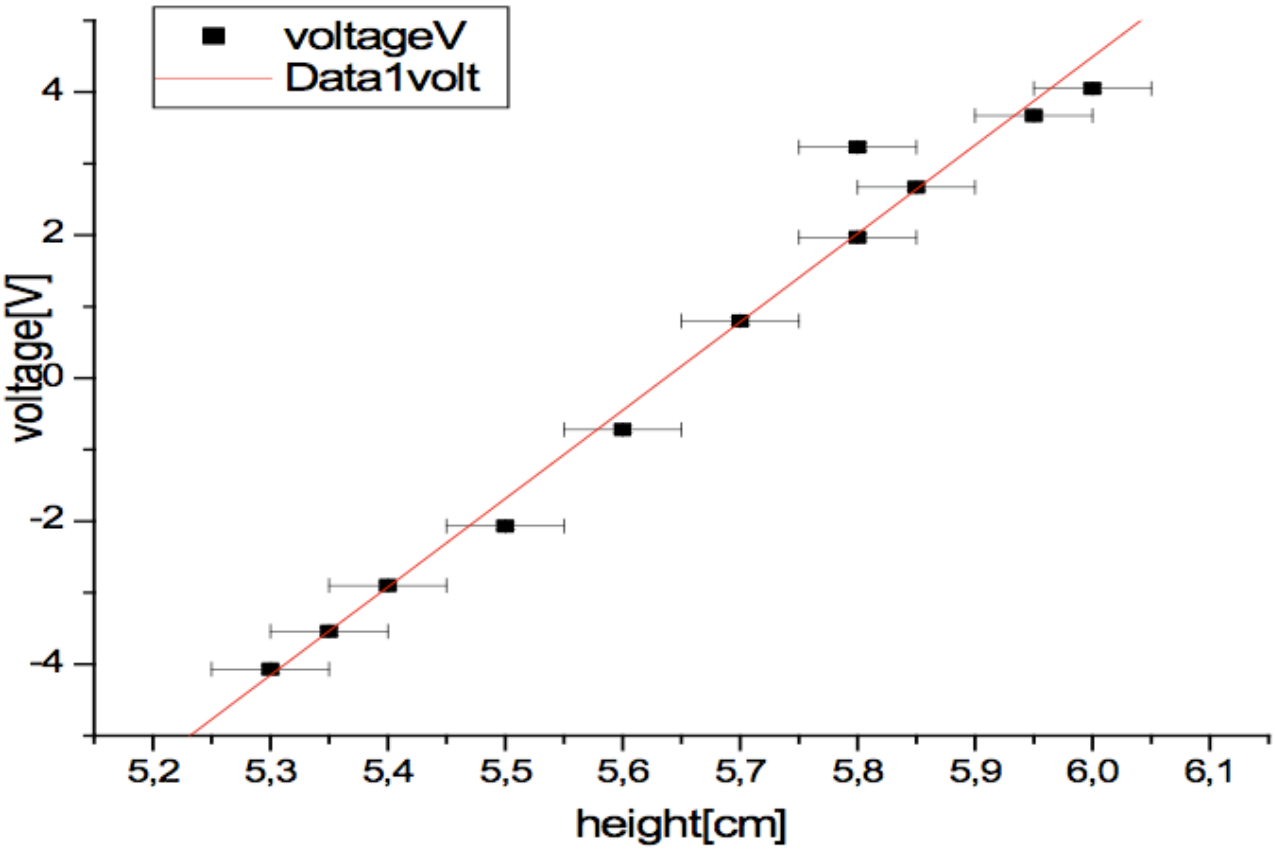

Fig.7:LVDT calibration

The linear range of our LVDT is between -4 and +4 volts. Applying a linear fit we can also obtain the conversion V/mm that is 1.236 V/mm.

Working Point

At fixed radial compression the vertical resonant frequency changes as a function of the equilibrium position (varying the payload weight) following, with very good approximation, a quadratic function. With optimal payload weight the GAS filter works at its minimum resonant frequency. To find this minimum we added again some coins on the load, excited the vertical oscillation and acquiring the LVDT signal. We analyzed the signal applying a damped-sinus fit and finding the oscillation frequency for every different load (see the example in fig.8, where the frequency is the fit parameter M2):

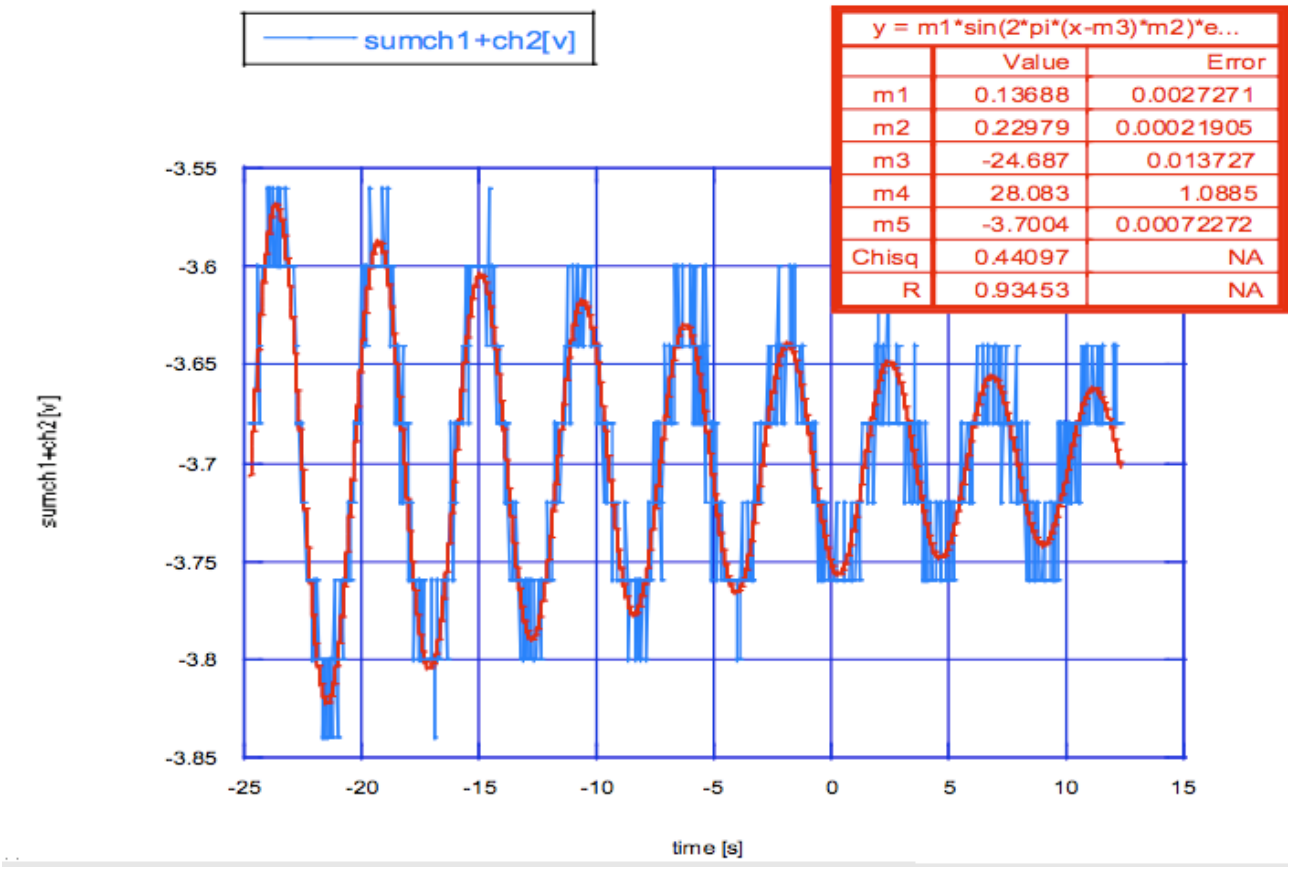

Fig.8:Damped-sinus fit of LVDT signal

The parabola obtained in this way is shown in fig.9.
From the fit results we obtained the minimum of this parabola. The miminum resonant frequency is around 0.194 mHz with the anti-spring settings that we used.
The frequency of the working point can be changed by changing the radial compression of the individual leaf springs.

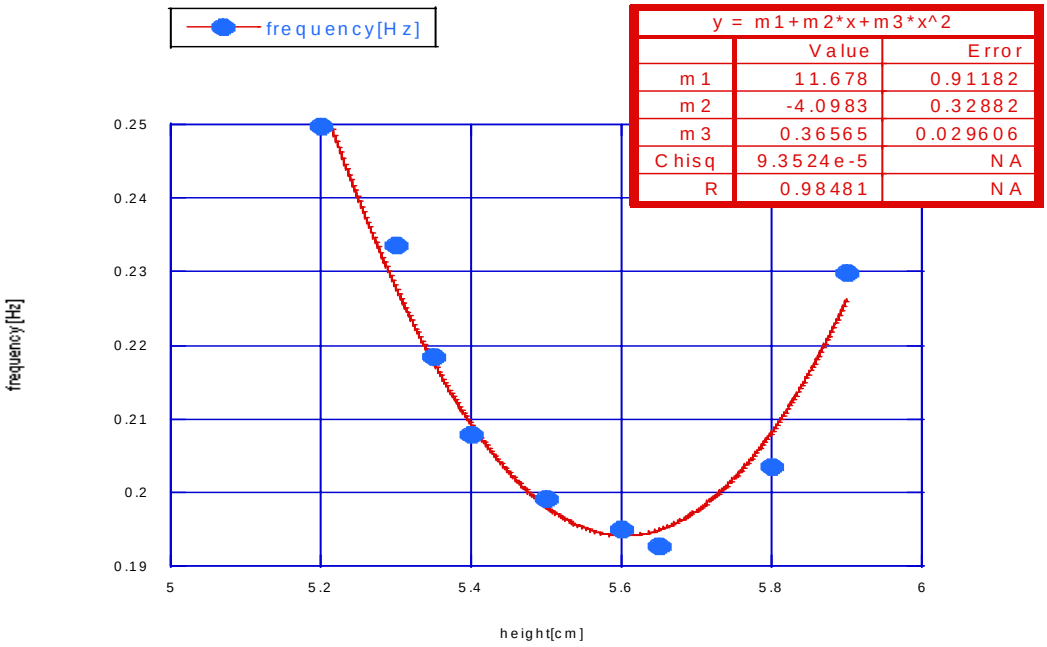

Fig.9:Vertical resonant frequency as a function of the payload weight

Actuator

To move the system we used a coaxial actuator positioned on the top of the GAS filter (fig.10,10.1).The actuator is a coil mounted into a loudspeaker magnet, normally driven by a sinusoidal signal with variable frequency.

Fig.10:Actuator on the top of the GAS filter

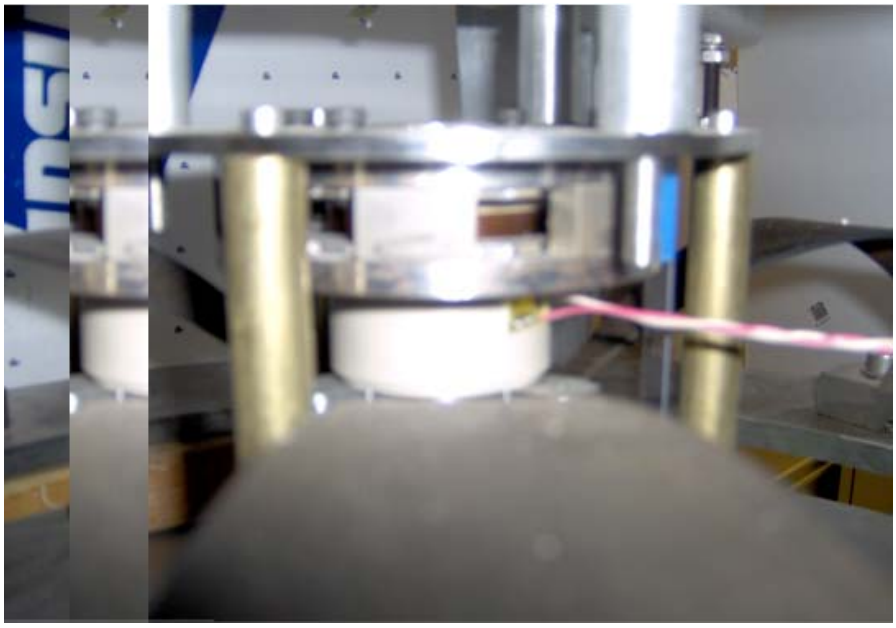

Fig.10.1:view of the coaxial actuator

In figure 10.2 is shown the calibration of the actuator driven with variable frequency.

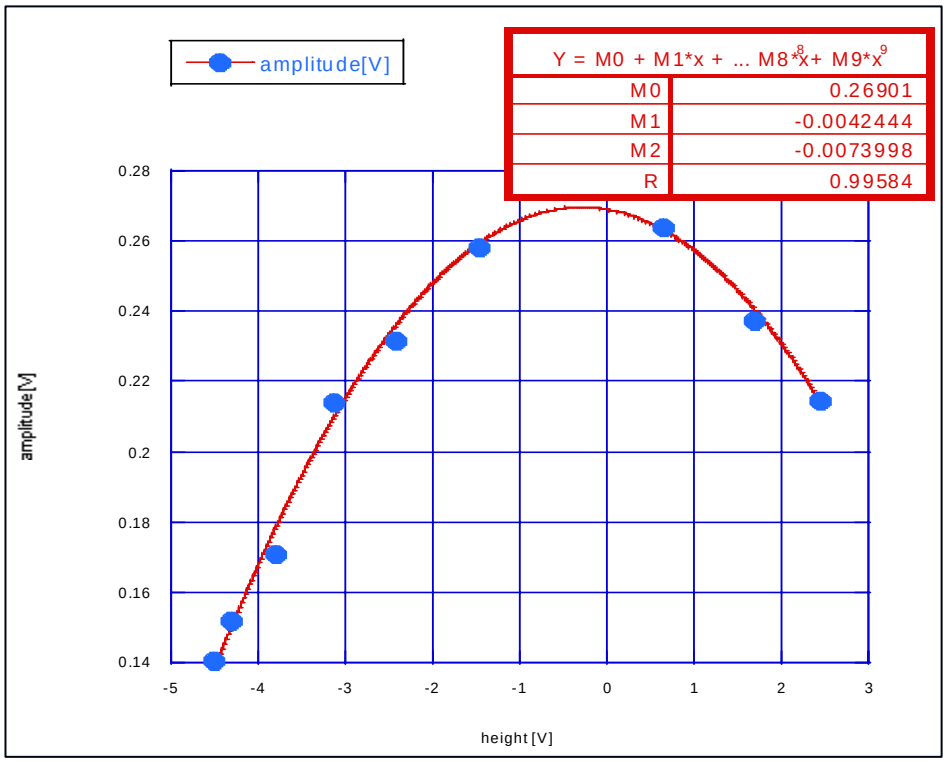

Fig.10.2:Actuator response.

Noise of the System

We observed the load moving under the effect of air conditioning, so we built a box around the GAS filter and studied the noise of the system with and without the box (fig.11).We acquired signal from LVDT sensor and we built a bar chart (*istogramma)* of voltage. Then we applied a gaussian fit and we estimated the air current system noise as the standard deviation of the fit (fit parameter M4). The noise obtained in this way is different in the case of the GAS filter with box around (0.19 mV=0.15 µm of noise, from LVDT calibration, fig.12) and without box (0.33 mV=0.27 µm ,fig.13).We decided to work always with the system closed inside the box.
The residual noise is due to seismic motion, thermal drifts, electronics noise etc. The thermal drifts will be eliminated by electronics feedback.

Fig.11:The box around GAS filter.

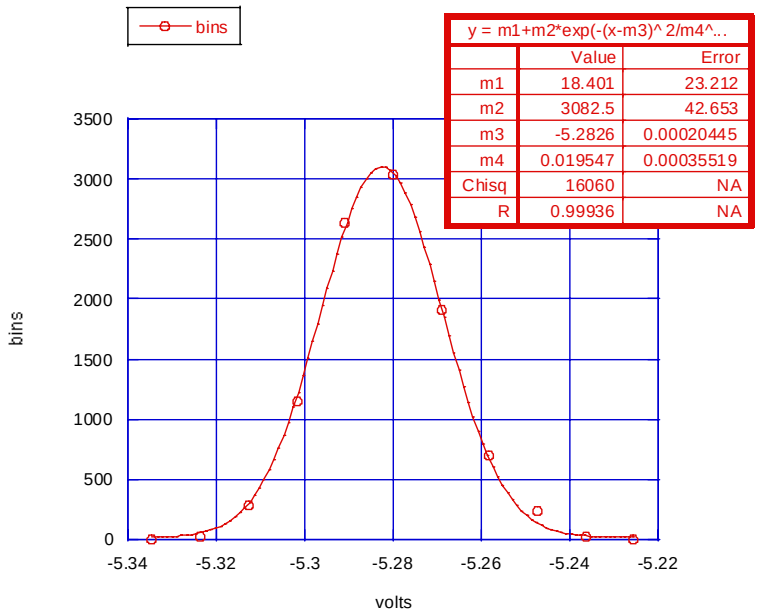

Fig.12:Gaussian fit of LVDT signal with box around GAS filter

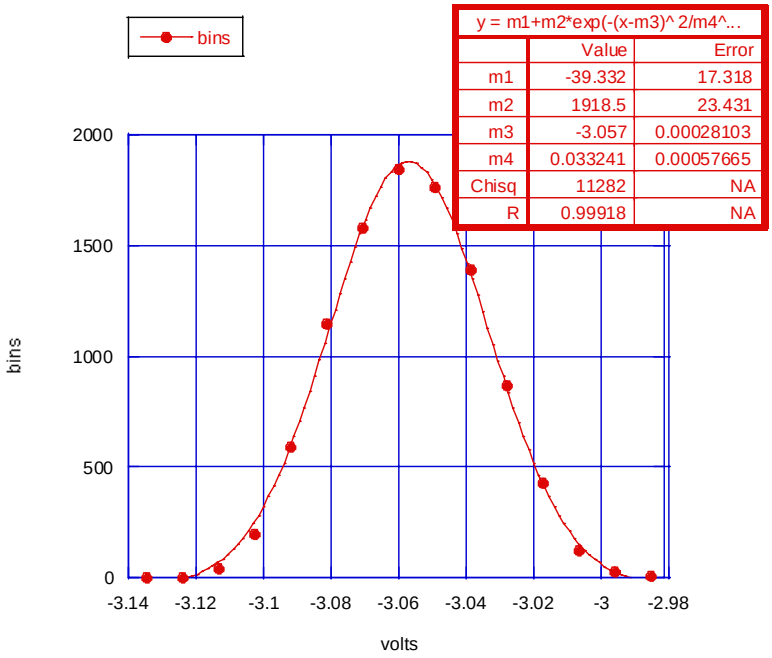

Fig.13:Gaussian fit of LVDT signal without box around GAS filter

First Measure of Hysteresis

The system was tuned around the minimum at 194 Hz. We worked with low frequencies of excitation, far from all resonant frequencies of the system, in order to isolate the hysteresis signal. We acquired 500 second of LVDT signal with the actuator driven at 10 mHz.
The plot of voltage obtained (LVDT) versus sinusoidal signal (actuator) is shown in fig.14:

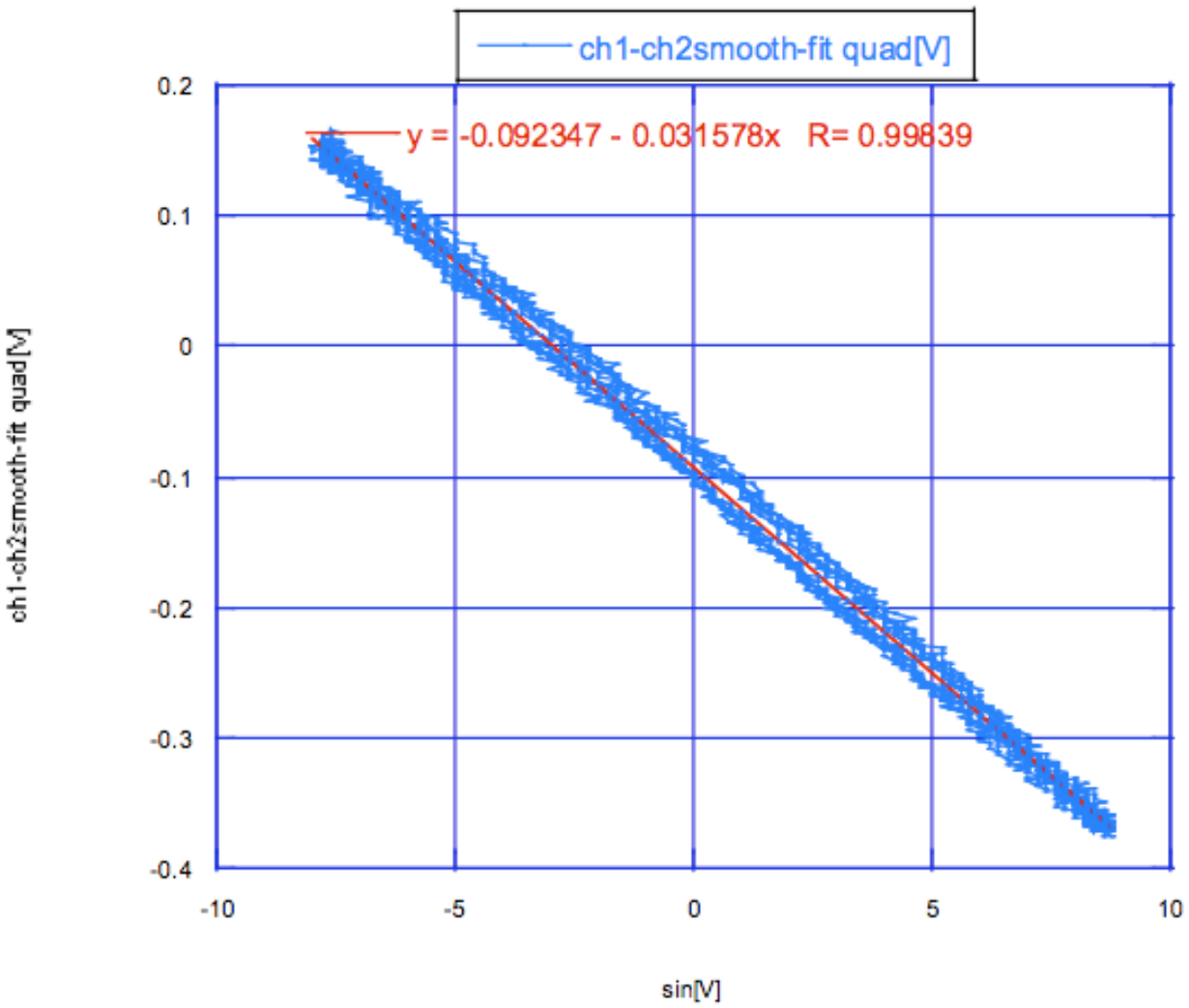

Fig.14:Linera fit of LVDT signal versus sinusoidal signal.

In order to have this plot in Newton vs meters we have to do some conversion.
The position is obtained from the conversion factor found in the LVDT calibration:
$X[mm] = LVDTsignal[V]/1.236\ \ [V/mm]$

The force applied is F=Kx with K= ω^2 m (f=0.194 Hz and m=64.52 kg).
The effective spring constant is K=95.87 N/m.
Building a plot of force vs sinusoidal signal and applying a linear fit we found the conversion N/V, in our case 0.0024493 N/V, as shown:

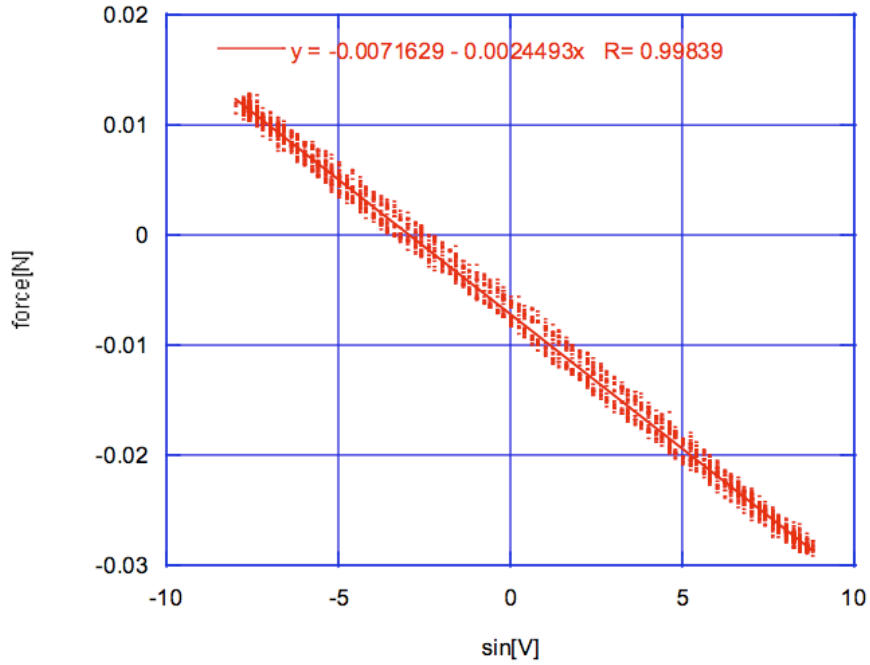

Fig.15:Linear fit of force versus sinusoidal signal.

Now we can have the final hysteresis loop:

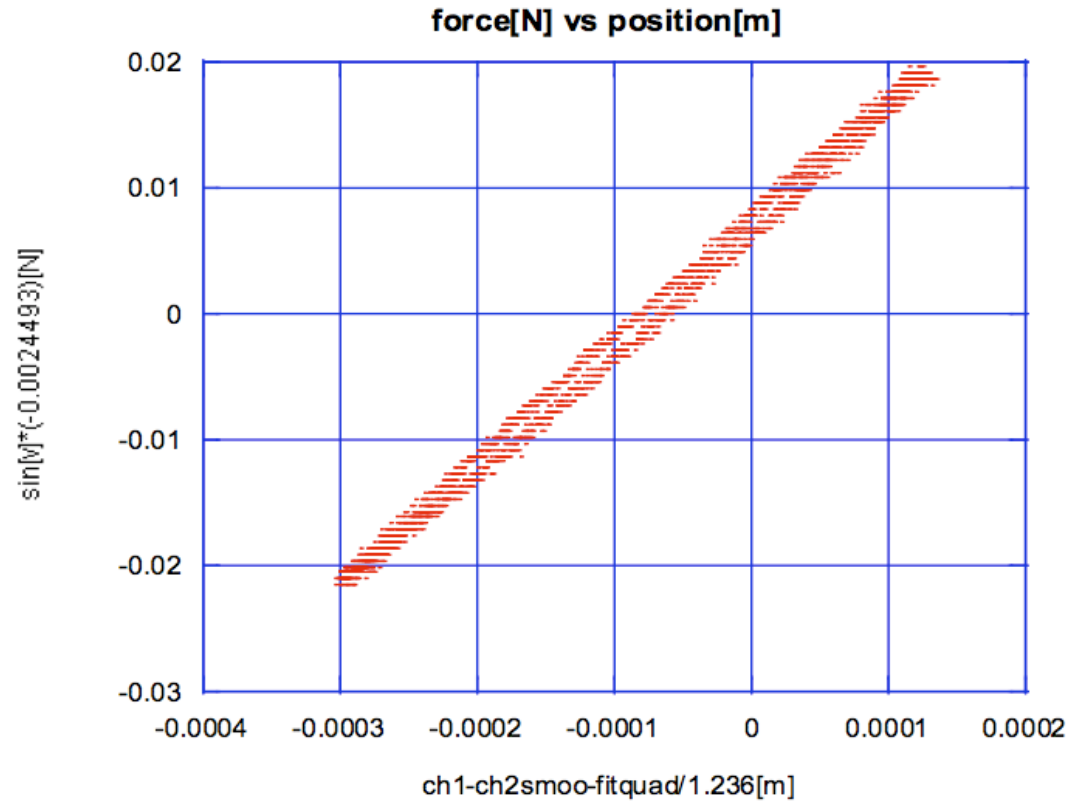

Fig.16:Hysteresis cycle [Joule].

The energy loss of the system, calculated from the area of this loop, is around 0.5μJ.
This value is compatible with the little displacement of the system under stress.

Acquisition Program

To further study the hysteresis we decided to sweep both frequency and amplitude of the sinusoidal signal injected in the system around the resonant frequency. We built a LabView program to acquire data from LVDT and we used a signal generator to drive the actuator. We found the voltage of the working point changing with temperature, so we built a position-set point integrator that we used in feedback with a time constant of hundreds of seconds on the actuator to stabilize the set point of the filter.
The acquisition program and set-point integrator program are shown in fig 17-18:

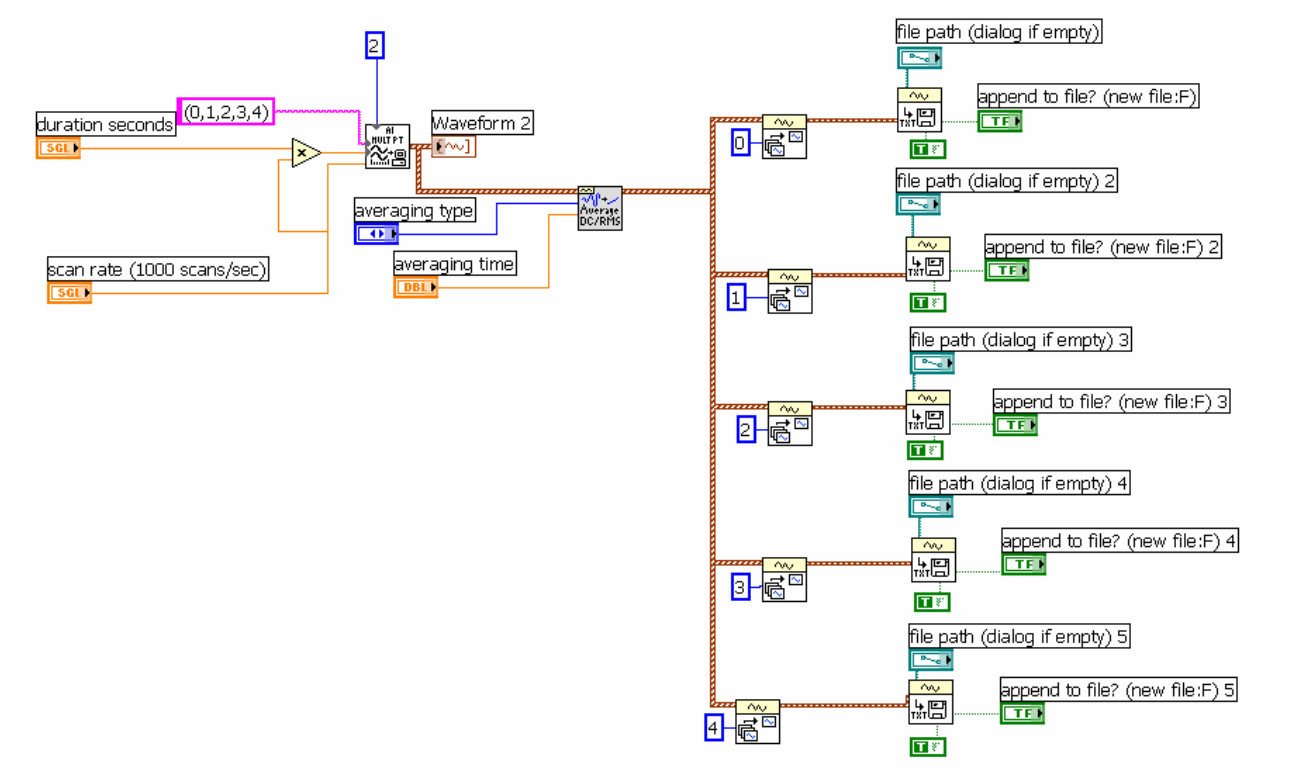

Fig.17: acquisition program

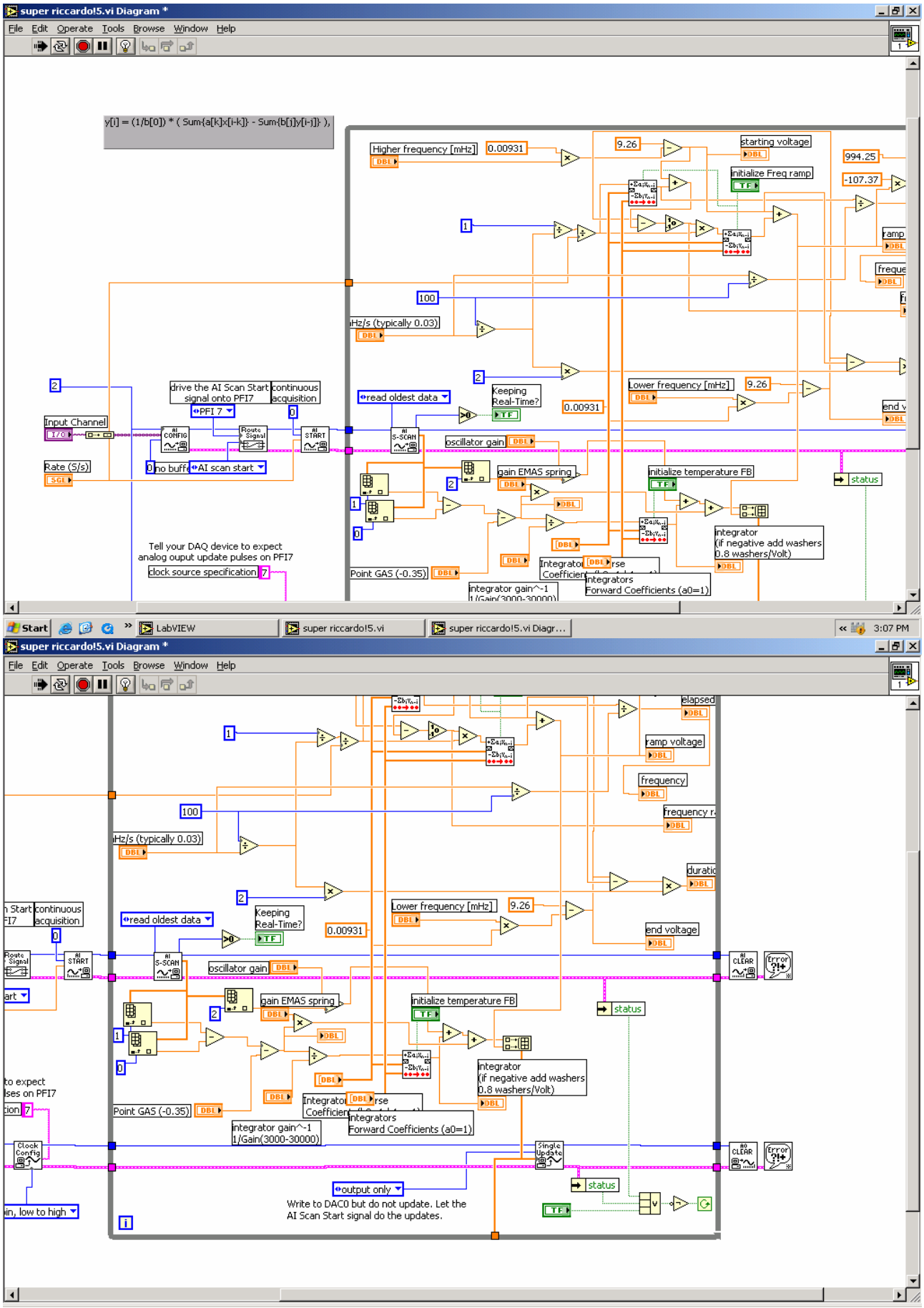

Fig.18: set-point integrator program.

The actuator is driven by a sinusoidal signal with variable frequency, in order to do a scan up and down in frequency around the resonance of the system.
We acquired a large amount of data of amplitude (LVDT signal) vs frequency (injected signal).
The phase of the signal is expected to change sign around the resonance, and this is what we obtained:

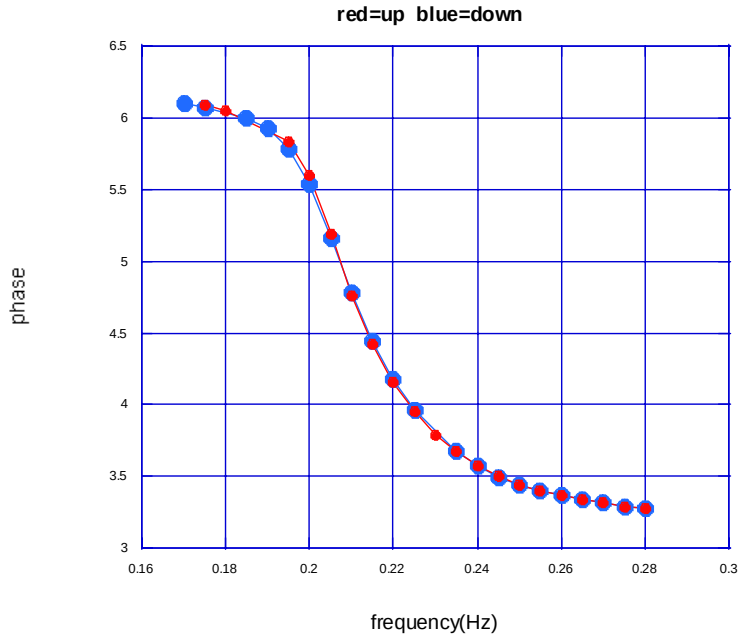

Fig.19: Phase of LVDT signal, for a frequency scan up and down.

The plot of amplitude vs frequency is instead shown in fig.20 for a resonant frequency of 210 mHz:

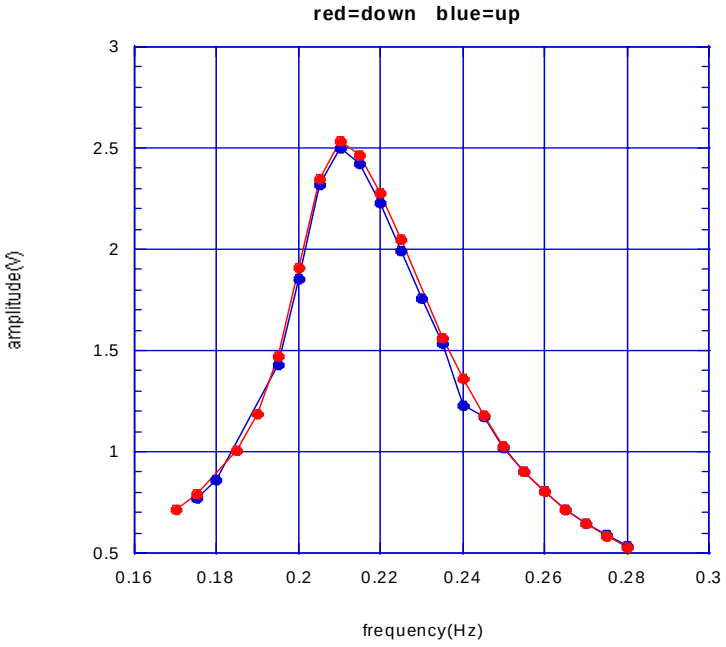

Fig.20: Amplitude of LVDT signal, for a frequency scan up and down.

The oscillation amplitude is greatest at the resonance, we see a peak around 210 mHz. The resonant frequency is shifted a little by the presence of the temperature feedback, which acts like a weak springs in parallel to the GAS spring. This effect will have to be carefully taken into consideration. For this reason the lost energy is maximum around resonance, and we see increasing hysteresis loop when we pass through resonant frequency:

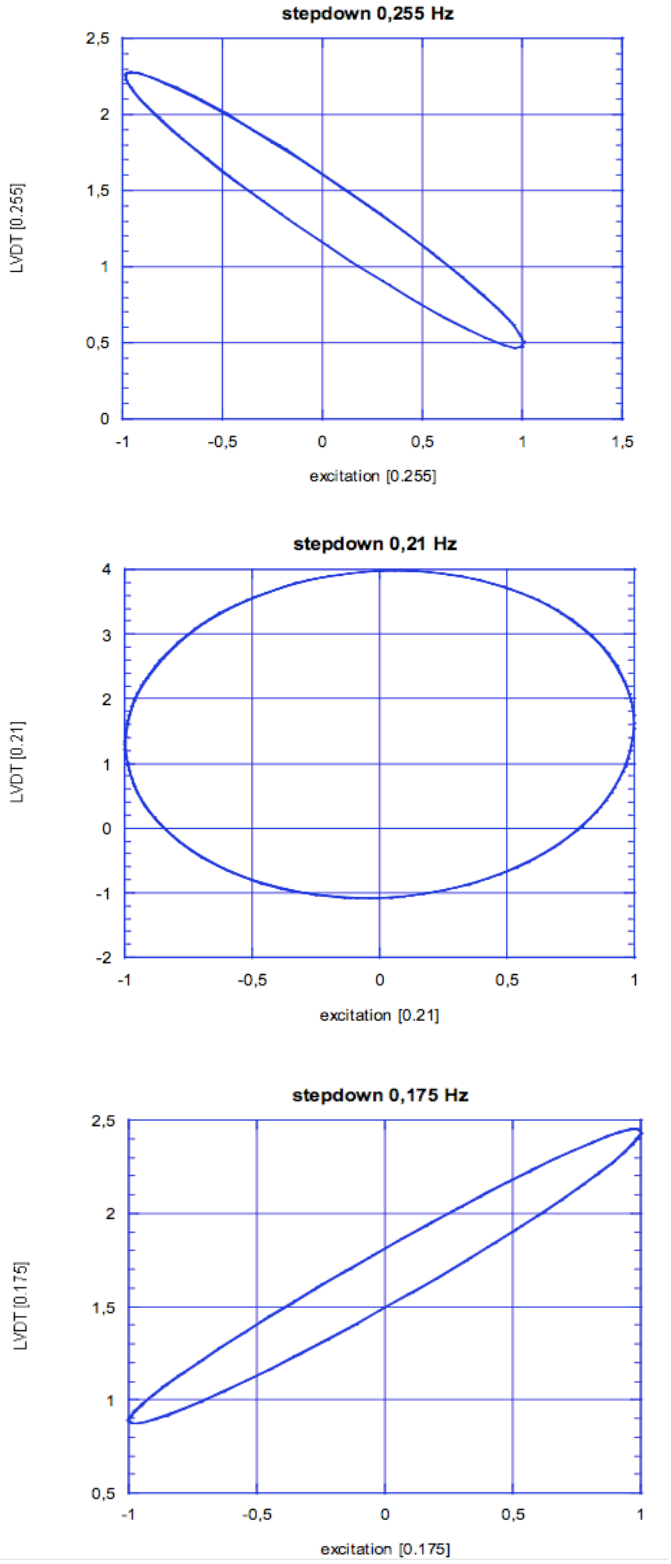

Fig. 21: From the upper panel: hysteresis loop before, through and after resonant frequency.

EMAS

In order to reduce the resonant frequency of our system, we added an electro-magnetic anti spring (EMAS) to the integrator program. It is a current applied to the actuator coil directly proportional to the movement of the payload from the working point. This anti spring force is added to the sinusoidal excitation signal and sent to the actuator. The EMAS is used to improve the signal to noise of our data, because the hysteresis effects are more evident at very low frequency when the system recalling forces are lowest. Changing the EMAS gain the smallest resonant frequency obtained in our test is around 80 mHz (Mantovani obtained 30 mHz in air while HAM SAS at LASTI rached 10 mHz in vacuum).
The plot of frequency vs EMAS gain is shown in fig.22:

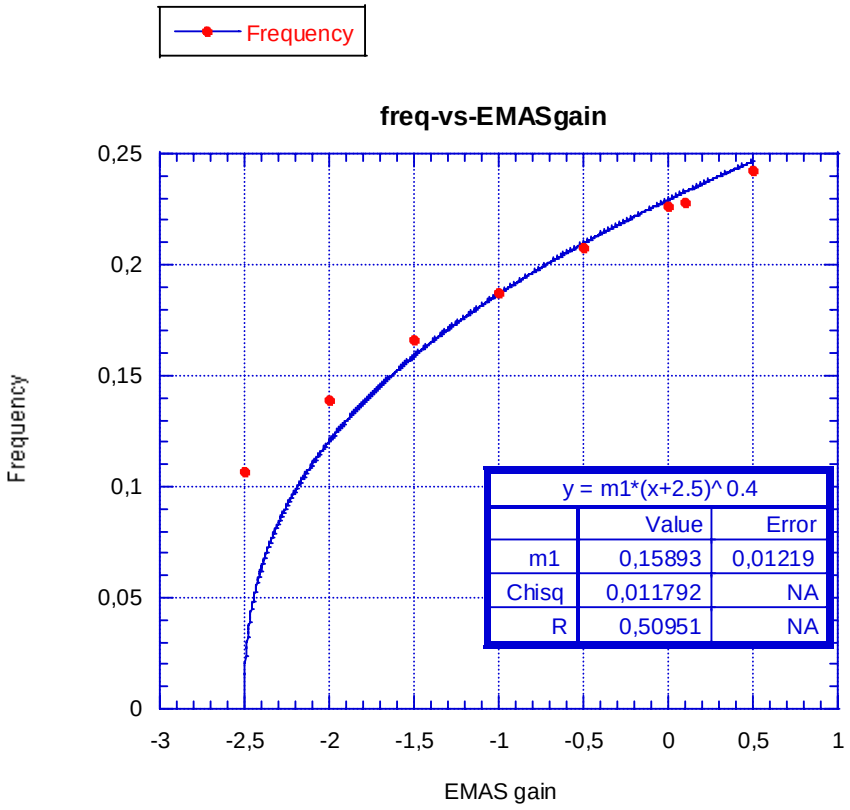

Fig.22: polinomial fit of frequency versus EMAS gain

For a gain of 0 we obtained the resonant frequency of the system without EMAS and for a gain of -2.5 the smallest resonant frequency of 120 mHz. With tuning of thermal integrator and higher gain 80 mHz was later obtained in this setup.
We acquired data changing both the EMAS gain and the amplitude of the signal injected in the actuator.
In the next figures plot of amplitude and phase of LVDT signal are shown, for different EMAS gain and sinusoidal signal amplitude:

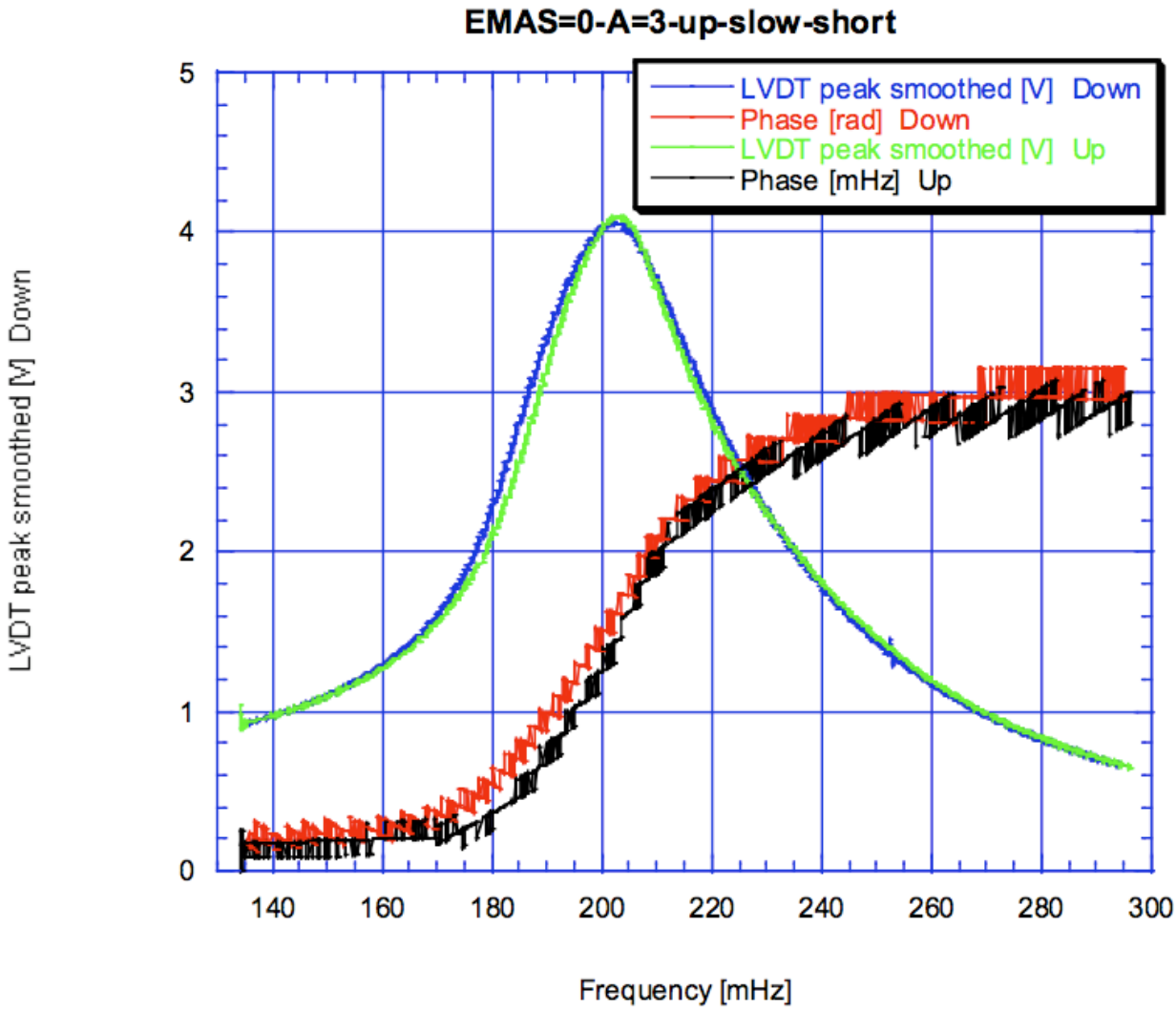

Fig.23:emas gain=0,amplitude=3V

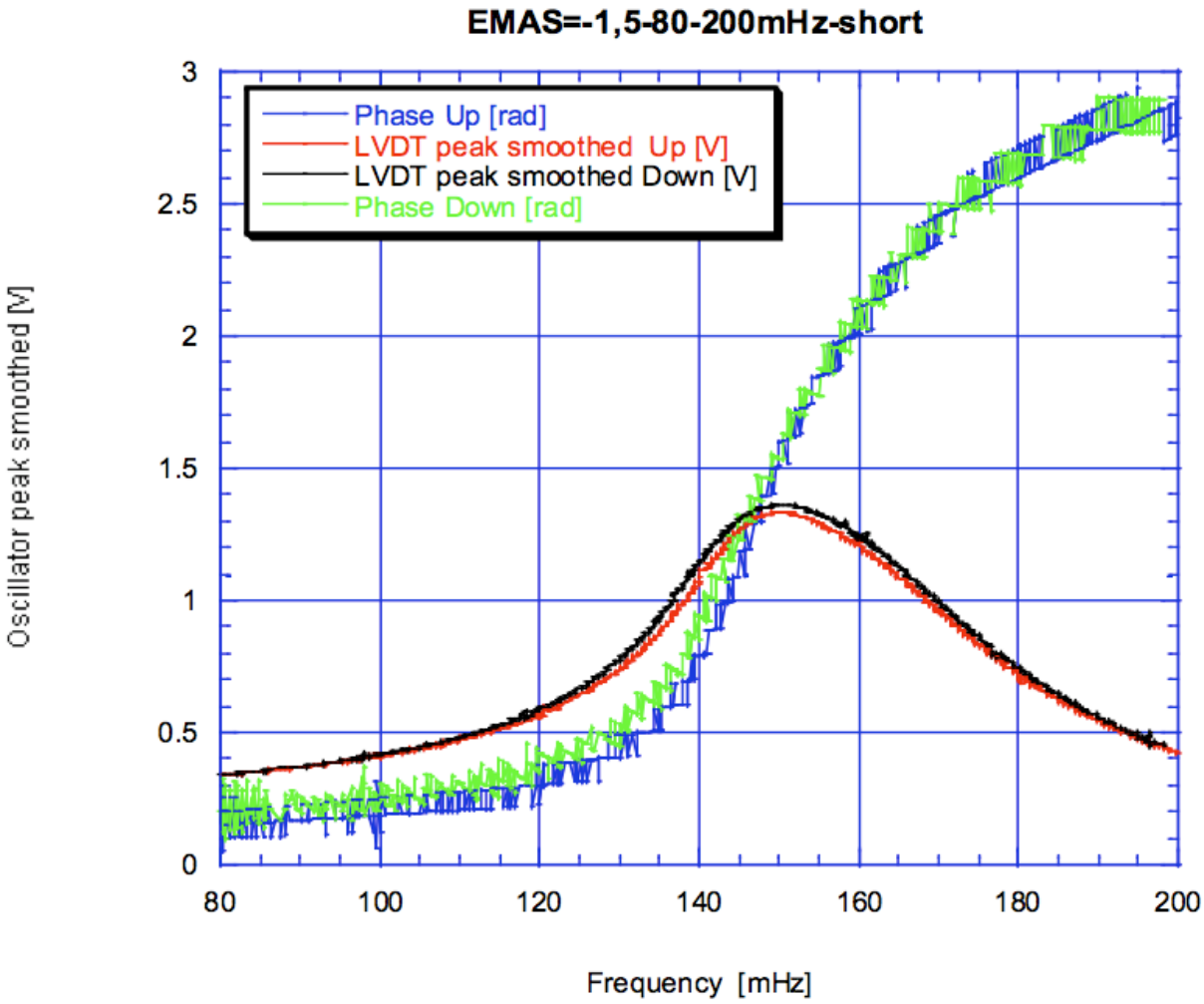

Fig.24:emas gain=-1.5,amplitude= 1V

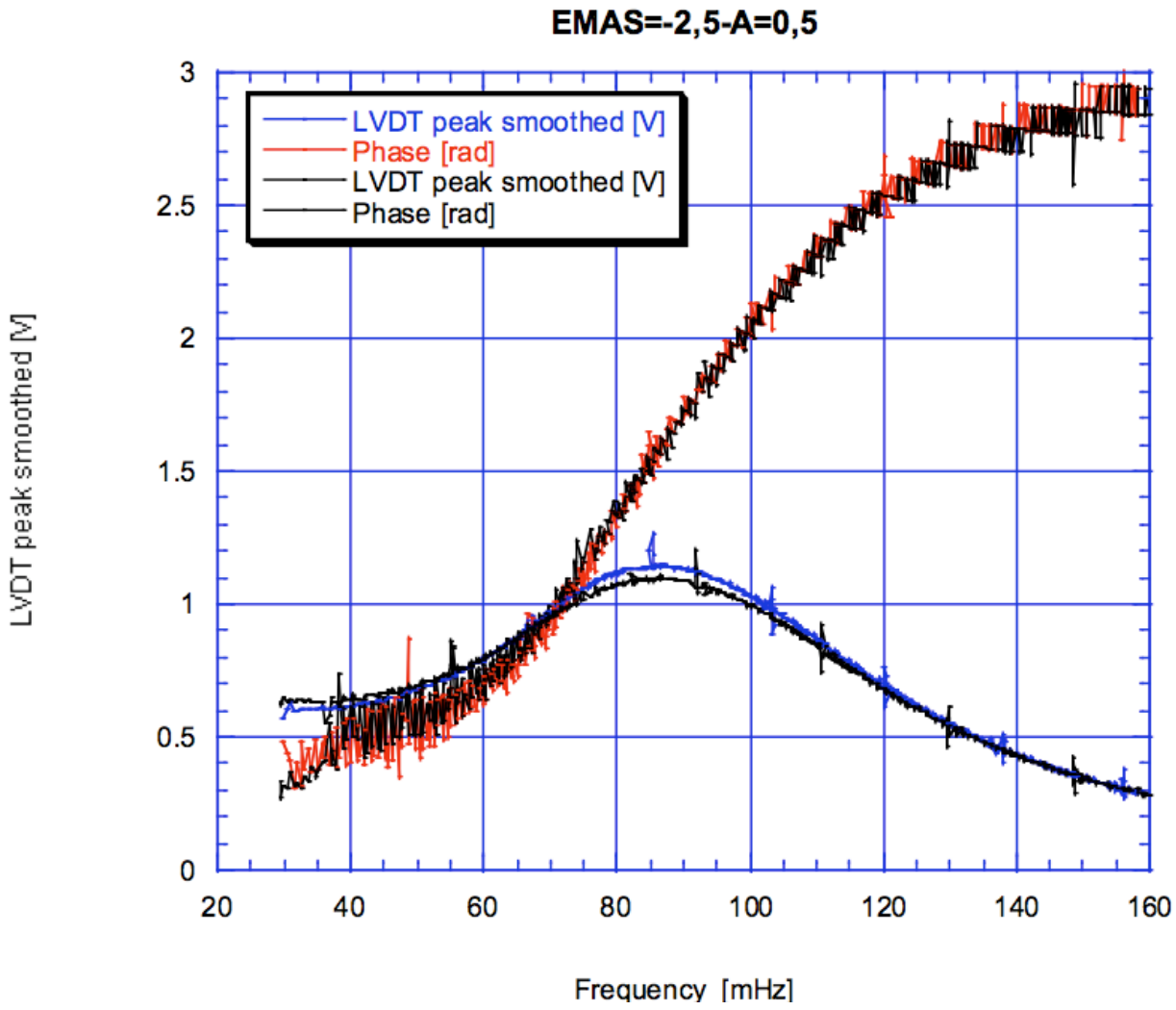

Fig.25:emas gain=-2.5,amplitude=0.5V

Conclusion

We expected to observe different behaviours in amplitude and phase with a frequency scan up and down, but these differences are not so evident in our data.
We noted a small difference in the amplitude plot between the sweeps up and down in frequency. This difference, more evident when the signal amplitude is high (3 Volt), may be compatible with an asymmetry expected in an hysteresis affected oscillator.
A frequency scan with amplitude greater than 3 V probably would improve this effect, if it was not for the case that the system, for higher oscillation amplitudes, starts being strongly non linear.
The hysteresis effect, related to the analysis of our data, is still under investigation.

Bibliography

A.Stochino,R. De Salvo, Y. Huang, V. Sannibale, *Improvement of the sismic noise attenuation performance of the Monolithic Geometric Anti Spring filters for Gravitational Wave Interferometric Detectors*, LIGO-P060044-A-Z

A.Stochino, *Performance Improvement of the Geometric Anti Spring (GAS) Seismic Filter for Gravitational Waves Detectors*, LIGO-T0500239-00-D

C.Wang, H. Tariq, R. De Salvo et al., *Constant force actuator for gravitational wave detector's seismic attenuation systems (SAS),*Nuclear Instruments and Methods in Physics Research A 489 (2002) 563-569

R. De Salvo, *Passive,non-linear mechanical structures for seismic attenuation*, LIGO-P050001-00-D

Acknowledgements

I would like to thank my mentor in the USA Riccardo De Salvo for everything: help, discussions, work, patience. I spent constructive days in Caltech with him.
I also want to thank my supervisor in Rome Prof. Fulvio Ricci who gave me the possibility to work at the California Institute of Technology.
My final thanks go to all the people and friends in (and out) Caltech who made this experience unique.